SUSTAINED SERVICE-LOAD BEHAVIOR OF CONCRETE BEAMS WITH RECYCLED CONCRETE AGGREGATES

Adam M. Knaack and Yahya C. Kurama

Biography: Adam M. Knaack is a design engineer at Schaefer in Cincinnati, OH. He received his Ph.D. and M.S. in civil engineering from the University of Notre Dame in Indiana, USA.

ACI member **Yahya C. Kurama** is a professor of civil engineering at the University of Notre Dame in Indiana, USA. He is a member of ACI Committees 555, 550, and 374.

ABSTRACT

This paper describes an experimental investigation on the time-dependent sustained service-load behavior of normal strength concrete beams with recycled concrete aggregates (RCA) used as replacement for coarse natural aggregates (NA). Eighteen beams were tested incorporating different aggregate replacement amounts, reinforcing details, concrete age at superimposed loading, and beams with and without cracking upon immediate load application. It is shown that increased amounts of RCA result in significant increases in both the immediate and long-term deflections of concrete beams, but this effect is smaller for beams with increased cracking. Greater creep and shrinkage deformations also cause a greater downward shifting of the neutral axis (i.e., increase of the neutral axis depth) in RCA concrete beams as compared to NA concrete beams. ACI 318 and Eurocode generally gave good design estimates for the immediate deflections of the test specimens. In comparison, the long-term deflections were significantly underestimated for the uncracked beams. For the cracked beams, the long-term deflections were somewhat underestimated by ACI 318 and overestimated by Eurocode by approximately similar percent errors. The ability of the design methods to predict the measured deflections did not differ significantly between the NA concrete and RCA concrete beams.

Keywords: beam deflections; neutral axis; RCA; recycled concrete aggregate; sustained load.

INTRODUCTION

This paper investigates the effect of RCA on the immediate and time-dependent sustained service-load behavior of 18 slender normal strength concrete beams tested under four point bending. The test specimens include beams with different amounts of coarse aggregate replacement (100, 50, and 0% replacement), with and without compression reinforcement, with and without cracking upon initial superimposed loading, and beams loaded at age of 7 days versus 28 days. The measured midspan deflections of the test specimens are presented and compared with design predictions from ACI 318[1] and Eurocode.[2] The neutral axis depths of the cracked beams are also reported. Full information about the research program and the test results, including the project report,[3] can be found at *www.nd.edu/~concrete/RCA-concrete/*.

RESEARCH SIGNIFICANCE

Previous research has shown that RCA has a greater effect on the stiffness than on the strength of concrete. There is also a large increase in the creep and shrinkage of concrete as a result of RCA. Thus, increased service-load deflections rather than reduced strength may be a greater limitation for RCA in structural applications (e.g., beams, columns). This paper focuses on this topic. By quantifying the effect of RCA on the deflections of reinforced concrete beams, it would be possible to consider the increased deflections in structural design (for example, by reducing the amount of RCA if the allowable deflections are exceeded).

BACKGROUND

There has been little previous research on the time-dependent sustained load deflections of RCA concrete beams,[4-7] and the results from these studies are generally limited to a few tests using RCA and one applied load level in each research program. Researchers have found that the

use of RCA greatly increases the beam deflections. For example, for a service-load duration of about 15 weeks, Lapko and Grygo[6] showed 20% greater deflections in RCA concrete beams with full (100%) aggregate replacement as compared to natural aggregate (NA) concrete beams. These tests were conducted on small-scale beams with a cross section of 3x5 in. (76x127 mm). Ajdukiewicz and Kliszczewicz[4] found similar results for RCA beams with full aggregate replacement loaded for up to one year. Choi and Yun[5] found the ratios of long-term to immediate deflections for RCA concrete beams to be smaller than the ratios for NA concrete beams.

In comparison, there has been a considerably larger body of previous work on the ultimate behavior of RCA concrete beams, during which the immediate deflections (i.e., initial stiffness) were also measured. The largest differences were noticed in the immediate deflections. For example, Li[8] reported that the immediate deflections under service level loads were about 10-24% larger for RCA concrete beams with full replacement as compared to NA concrete beams. Sato et al.[7] reported that the well-known ACI 318[1] equation for the effective moment of inertia could be used to reasonably predict the immediate deflections for RCA concrete beams with full replacement at low load levels, but that this equation was unconservative at higher loads.

Previous work[9-18] on material properties has shown that RCA concrete has decreased compressive strength, decreased modulus of elasticity, and increased creep and shrinkage strains as compared to NA concrete. These effects have been found to be greatest for the modulus of elasticity and smallest for the strength, and have been generally attributed to the residual mortar attached to the coarse natural aggregate in RCA, which results in increased porosity, increased absorption, and reduced mechanical resistance, as well as weaker interfacial transition zone.

EXPERIMENTAL PROGRAM

All 18 beams were l=4.0 m (13 ft) long, b=150 mm (6.0 in.) wide, and h=230 mm (9.0

in.) deep, with two different reinforcement layouts. One layout [UT Series, **Fig. 1(a)**] had only tension longitudinal steel bars, while the other layout [UC and CC Series, **Fig. 1(b)**] had compression longitudinal bars and transverse hoops in addition to the tension longitudinal bars. In the specimen nomenclature, the first letter "U" indicates beams that were not intentionally cracked under the applied superimposed load whereas the first letter "C" indicates beams that were subjected to a greater superimposed load to induce immediate cracking. For the second letter of the nomenclature, the letter "T" indicates beams with only tension longitudinal steel bars and "C" indicates beams with compression longitudinal bars and transverse hoops in addition to the tension longitudinal bars. The main bottom (tension) longitudinal reinforcement in both layouts consisted of two No. 16 (U.S. No. 5) Grade 420 (U.S. Grade 60) bars. The top (compression) longitudinal and transverse steel in the UC and CC Series beams consisted of two No. 10 (U.S. No. 3) Grade 420 bars and No. 10 Grade 420 rectangular hoops at 95 mm (3.75 in.) spacing, respectively. Six beams were cast in each of the CC, UT, and UC Series.

Concrete Aggregates

INDOT[19] No. 23 "concrete sand" was used as fine aggregate and crushed limestone (NA-CL) from a local ready-mix concrete plant was used as natural coarse aggregate. The RCA was from a local construction/demolition recycling plant. While this facility receives debris from many sources, the RCA used in this project (RCA-S) was made from the demolished foundation of a late 1920s manufacturing plant in South Bend, Indiana. The coarse natural aggregate and RCA satisfied INDOT[19] No. 8 gradation requirements with a nominal maximum aggregate size of 19.0 mm (3/4 in.).[3] All aggregates, including the RCA, were available in this gradation with no additional processing because of the common use of INDOT No. 8 aggregate in Indiana.

Table 1 shows the properties of the aggregates. The specific gravity and absorption were

determined using ASTM[20] C127 and C128 for coarse and fine aggregates, respectively. The residual mortar content, RM_{rca}, which is a measure of the percent (by weight) of residual mortar in the RCA, was determined as described in Abbas et al.[21] The deleterious material content, D_{rca}, provides the percent (by weight) of the deleterious substances in the RCA. Because RCA-S came from a demolition, there was some brick, asphalt, and wood in the material. These substances were identified (but not removed) by visual inspection of the RCA retained on a 9.50 mm (3/8 in.) sieve during washing as well as after oven drying (which resulted in color variations of the bituminous materials). The L.A. abrasion loss was determined per ASTM[20] C131.

Concrete Mix Design and Preparation

One target NA concrete mix design and two RCA concrete mix designs utilizing the direct volume replacement (DVR) method were used. The DVR method simply replaces a volume of coarse NA with an equivalent volume of RCA according to **Eq. 1**:

$$R = 1 - V_{NA}^{DVR}/V_{NA}^{NAC} \quad (1)$$

where, R=volumetric replacement ratio for coarse aggregate; V_{NA}^{DVR}=volume of NA in DVR mix; and V_{NA}^{NAC}=volume of NA in natural aggregate concrete mix. Thus, for a given volume of concrete, the volumetric proportions of the total coarse aggregate (RCA plus NA), fine aggregate, cement, and water remain constant between the different DVR and NA concrete mix designs.

Table 2 shows the dry-weight proportions of the three mix designs corresponding to R=0%, 50%, and 100%. The R=0% mixes were used as the target NA concrete (i.e., benchmark conventional concrete), the R=100% mixes investigated full aggregate replacement, and R=50% was selected as an intermediate level replacement. The target NA concrete had a water-to-cement (*w/c*) ratio of 0.44 for an approximate target 28-day strength of 40 MPa (6000 psi), slump of 125±25 mm (5±1 in.), and air content of 5.0±1.5%. The cement was ASTM[20] C150 Type I

portland cement, and an air-entraining agent (AEA) and high-range water reducer (HRWR) satisfying ASTM[20] C260 and C494 (Types A and F), respectively, were also used.

All coarse RCA and NA was washed and then oven-dried for consistent weighing. The sand was not washed but it also was oven-dried and weighed. At least 19 hours before casting, all aggregates (including sand) were saturated with water. Then, the excess water was decanted and the aggregates were weighed again. Using the absorption values in **Table 1**, the amount of water in excess of the saturated surface dry (SSD) condition was subtracted from the total mix design water in **Table 2** to determine the added water to achieve the desired *w/c* ratio. Note that the aggregate drying and pre-soaking process above is not intended for commercial applications but rather it was used in this research to consistently control the amount of free water in each mix.

Concrete Casting and Curing

The beams were cast in their as-tested (i.e., upright) configuration. One 4.0 m (13 ft) long beam, a number of companion concrete strength and stiffness test cylinders, and modulus of rupture (MOR) test specimens were cast from each concrete batch mixed in a 0.34 m^3 (12 ft^3) rotating drum mixer [batch sizes ranged from 0.19 to 0.23 m^3 (6.8 to 8.0 ft^3)]. Three beams were made on each casting day, corresponding to R=0%, 50%, and 100%. ASTM C192 requirements for mixing concrete in the laboratory were generally followed. The only exception was that all of the mix water was first added to the mixer along with the liquid admixtures. With the mixer turning, the coarse and fine aggregates were added simultaneously and then the cement was added slowly to ensure proper mixing. Once all the materials were in the mixer, the concrete was mixed for three minutes, allowed to rest for three minutes, mixed again for two more minutes,[3] and immediately placed in the formwork. The test beams and companion MOR specimens were moist cured under plastic sheeting for two days, and then removed from their forms to be stored

inside the laboratory air until testing. The companion material test cylinders were also de-molded and allowed to cure under the same laboratory air conditions after two days from casting.

Test Setup, Procedure, and Schedule

As shown in **Fig. 2**, each l=4.0 m long (13 ft) beam was subjected to four-point bending using concrete weight blocks to simulate superimposed service loads for a period of at least 119 days. The clear beam span between simple supports was l_n=3.7 m (12 ft), resulting in a clear span length to depth (l_n/h) aspect ratio of 16 (which is the same as the aspect ratio limit for simply supported beams in ACI 318[2] Table 9.5a). The superimposed load was applied at ±190 mm (7.5 in.) on either side of the beam midspan by placing each weight block on two steel shims. To apply the load, the weight block was first placed on four screw jacks, which were then lowered slowly and uniformly until the block would touch down on the beam with little impact.

Two different superimposed load block sizes were used such that the smaller block would not cause concrete cracking in the beam upon initial placement of the load (UT and UC Series beams) while the larger block would cause flexural cracking upon immediate loading (CC Series), but the steel in tension and the concrete in compression would remain in the linear-elastic range. The selected weights of the small and large blocks, as measured using a calibrated load cell, were P=371 and 971 kg (817 and 2140 lbs), respectively, which corresponded to approximately 75% of the predicted (using reinforced concrete mechanics) cracking load and 65% of the predicted linear limit load (governed by concrete reaching $0.45f_c'$ in compression), respectively. The surfaces of the load blocks were sealed with two coats of masonry water-proofer and two coats of paint to maintain a consistent weight by minimizing moisture loss.

Due to laboratory space limitations, the beams were tested in three rounds. In each round, three beams (with R=0%, 50%, and 100% and cast on a given day) were loaded at age, t_0 of 28

days and three beams (again with R=0%, 50%, and 100%, but cast within 1 to 9 days later) were loaded at t_0=7 days. These loading ages are generally considered as standard for concrete testing. The first two sets of six beams were loaded for 119 days (about 4 months), and the last set of six beams was loaded for 170 and 226 days (about 5.5 and 7.5 months) at ages of t_0=28 days and 7 days, respectively. Among the last six beams, the small weight blocks removed from Specimens UC-0-28, UC-50-28, and UC-100-28 at the end of the 170-day loading period were placed in addition to the other weight blocks on Specimens CC-0-7, CC-100-7, and UC-50-7, which were tested for another 56 days, resulting in a total superimposed load duration of 226 days .

As shown in **Table 3**, the test variables included the superimposed load, P, aggregate replacement ratio, R, age at superimposed loading, t_0, and reinforcing details. Considering that the specimens were stored indoors, only minor changes in temperature occurred except for a few days when the laboratory doors were open to the outside weather [**Fig. 3(a)**]. The humidity measurements showed greater variations [**Fig. 3(b)**]. However, because all of the specimens in each test series were exposed to the same temperature and humidity conditions, direct comparisons between the mixes with R=0, 50, and 100% in each series could be made.

Beam Measurements and Data Acquisition

The midspan deflection was measured and recorded using a string potentiometer and a data-logger. The string potentiometer was attached to the underside of each beam at the middle of the beam width so as to minimize any effects from accidental torsional deformations of the specimen. The measurements were taken every two seconds during and for at least the first hour after superimposed loading, then every fifteen minutes for the remainder of the testing duration.

Side surface deformation measurements were also taken at the midspan of each beam so that a strain distribution could be determined to show changes in the neutral axis depth under

load over time. To accomplish this, small brass inserts[3] (Humboldt Manufacturing H-3230.3), similar to those used in concrete creep and shrinkage measurements according to ASTM C512, were placed in two vertical lines along the depth of the beam and spaced ±76 mm (±3.0 in.) from the midspan (**Fig. 4**). Each line consisted of eight inserts, with the top and bottom inserts placed 25 mm (1 in.) from the top and bottom of the beam, respectively, and 25 mm on center between the inserts. The strain measurements were taken by measuring the horizontal deformations between corresponding locations (i.e., insert pairs across a gage length of 152 mm) along the two lines of inserts using a mechanical dial gage[3] (Humboldt Manufacturing H-3230). An *Invar* master bar[3] (Humboldt Manufacturing H-3230.5) was used to calibrate the dial gage before and after each set of measurements. The manufacturer specifies an *Invar* bar to calibrate the dial gage because the material essentially undergoes no expansion or contraction with temperature changes. The strain measurements were initialized (i.e., zeroed) prior to the superimposed loading of each beam, followed by measurements immediately after loading, then once a day for the first three days, once a week for the first month, and once a month for the remainder of the loading duration.

The measurement variability (i.e., error) in the strains was determined through a series of repeated readings along the same pair of inserts. It was found that while the measurement errors were small relative to the ultimate strains towards the end of the loading duration, the smaller strains at the beginning of each test could have been affected by these errors. To reduce the amount of this variability, the reading across each pair of inserts was repeated three times and the strain was taken as the average value from these three measurements.

Concrete and Reinforcing Steel Properties

Average concrete and steel material properties were measured from a minimum of three samples for each concrete mix and steel type (see **Tables 4** and **5**). The concrete material tests

were conducted similar to the tests in Knaack and Kurama.[14] The compression strength, f_c' and modulus of elasticity, E_c were determined from 75x150 mm (3x6 in.) cylinders according to ASTM[20] C39. The modulus of elasticity was determined as the secant modulus between two points on the measured stress-strain curve [via an Epsilon© 3542RA extensometer[3] with 50 mm (2 in.) gauge length], with the first point at a strain of 0.00005 and the second point at a stress of $0.40f_c'$. The tension strength, f_t' was measured from modulus of rupture tests per ASTM[20] C293.

Fig. 5 plots the trends from the concrete material tests as average results from all of the beam specimens at each *R* ratio (average from total of six beams for each *R*), with the average results for each beam (average from three material samples) also shown. Because of the small number of *R* values, the lines connecting the data points at each *R* do not necessarily suggest a relationship, but rather help visually distinguish the different sets of data. Increased *R* resulted in large decreases in E_c and f_t', while the effect on f_c' was small. As expected, f_t' at a concrete age of 28 days tended to be greater than that at 7 days; however, there was no clear increase in f_c' or E_c with increasing age. In some cases, there was even a drop in the concrete mechanical properties with age, especially for E_c. The reasons for these conflicting trends are not known; however, in addition to the inherent variability in the concrete properties, air-curing of the cylinders following de-molding two days after casting could have limited hydration. Even though all beams with the same *R* were made using the same concrete mix design, there was significant variability in the strength and stiffness of concrete cast at different times. Different rates of water evaporation and cement hydration due to different temperature and humidity conditions at the time of casting could have affected the concrete strength and stiffness.[22]

All of the reinforcement used in the beam specimens was ASTM A615 Grade 60 steel and all bars of the same size came from the same manufacturing heat. ASTM[20] A370 standards

were used to determine the stress-strain behaviors of the No. 16 and No. 10 bars in tension [**Figs. 6(a) and 6(b)**]. The steel strains were measured using an MTS Model 634.25E-24 extensometer[3] with 50 mm (2 in.) gauge length. To prevent damage to the sensor, the extensometer was removed after a 0.5% drop in stress beyond the ultimate (peak) strength, f_u of the steel. The incremental strains following extensometer removal were calculated from the differential position of the test machine crossheads assuming that non-specimen deformations were negligible after the attainment of f_u . All bars had a distinct yield point, which was used to determine the yield strength, f_y and yield strain, ϵ_y . The modulus of elasticity, E_s was determined as the secant modulus between steel stresses of 34.5 and 68.9 MPa (5.0 and 10.0 ksi). The fracture strain, ϵ_f was taken as the strain at 20% drop from f_u (i.e., at a stress of f_f=0.80f_u).

RESULTS

Midspan Deflection

Fig. 7 plots the midspan deflection versus time behavior of each beam from application of superimposed load, through load removal, and subsequent deflection recovery. Deflection data for Beams UT-100-7 and CC-50-28 are not shown due to string potentiometer malfunction. Increased *R* resulted in significant increases in both the immediate and long-term deflections, but this effect was smaller for beams with increased cracking (which would be expected because of the smaller effect of concrete on a cracked beam than on an uncracked beam). For example, at 119 days, **Fig. 7(e)** shows that the uncracked beams with compression steel experienced a deflection increase of about 49% from *R*=0% to 100%. In comparison, again at 119 days, the cracked beams in **Fig. 7(d)** showed a smaller increase of about 21% from *R*=0% to 100%.

Similar to NA concrete beams, deflections of the RCA concrete beams were affected by loading age, compression steel, and cracking. Beams loaded at t_0=7 days tended to have larger

long-term deflections than their 28-day counterparts [e.g., **Fig. 7(e)** versus **Fig. 7(f)**]. Uncracked beams with compression steel had reduced long-term deflections than uncracked beams without compression steel [e.g., **Fig. 7(b)** versus **Fig. 7(f)**]. Lastly, as expected, cracked beams had significantly greater deflections than uncracked beams [e.g., **Fig. 7(c)** versus **Fig. 7(e)**].

Cracking

In the CC Series beams, distributed hairline flexural cracks developed (immediately upon superimposed load application) within the middle of each beam from approximately quarter point to quarter point along the span, with minimal cracking beyond this region.[3] **Figs. 8(a)** and **8(b)** show examples of flexural cracking on Beams CC-0-7 and CC-100-7, respectively. Note that the cracks remained hairline size and were highlighted by markers for ease of viewing. The flexural cracking in Beam CC-100-7 (with R=100%) extended further over the height than in Beam CC-0-7 (with R=0%). Increased cracking in the RCA concrete beams was expected due to the decrease in the modulus of rupture with increased R (**Table 4** and **Fig. 5**).

Fig. 8(c) shows a sample UC Series specimen (Beam UC-50-7), which also experienced cracking. Since the UC Series beams were loaded with the small weight blocks, no flexural cracking was observed upon initial load application. However, all of the beams in this series showed some flexural cracking over time during testing, likely as a result of the internal stresses that developed between the shrinking/creeping concrete and the reinforcing steel. As would be expected due to the smaller superimposed load, the extent of cracking over the height and length of the UC Series beams was significantly less than that in the CC Series beams. Unlike the UC Series, no cracking was visually observed in the UT Series beams.

All UC and CC Series beams with compression steel developed shrinkage cracks prior to the superimposed load application [e.g., see **Fig. 8(d)** for the shrinkage cracking in Beam UC-

100-28]. These cracks were generally only observed on the top surface of the beams and at most extended to the level of the compression bars [13 to 25 mm (0.5 to 1 in.) deep from the surface].

Neutral Axis Depth

Fig. 9 shows the total concrete strain diagrams over the height of the CC Series beams as determined from the horizontal deformation measurements between the two mechanical dial gage insert lines spaced ±76 mm (±3.0 in.) from the midspan. The thin to thick lines represent the strain diagrams beginning from the initial application of the superimposed load at time, t=t_0 and ending after 119 days of loading. Note that while some of the beams were left loaded beyond 119 days, the deformations at time, t=t_0+119 days are used herein for consistent comparisons. Also note that the diagrams in **Fig. 9** are for the total strain, ϵ_{total} (i.e., sum of mechanical, creep, and shrinkage strains), and not just the mechanical strain (thermal strains were small because of relatively little temperature variation in the lab as shown in **Fig. 3**). Also, because the dial gage measurements were initialized immediately prior to the superimposed loading, the results represent the increment of total strain from the initial application of the superimposed load at t=t_0. As a result, the concrete shrinkage strains from the initiation of drying or the creep strains from the beam self weight that accumulated until t=t_0 are not included in the measurements.

The results in **Fig. 9** show a significant lowering (downward shift) of the neutral axis (defined as the point of zero total strain) from the time dependent effects of creep and shrinkage. Since the point of zero total strain does not represent zero mechanical strain, the concrete stress was not zero at the neutral axis. An increase in R tended to result in further lowering of the neutral axis because of the increased creep and shrinkage of RCA concrete. The lowering of the neutral axis was smaller for beams loaded at t_0=28 days than beams loaded at 7 days. This trend can be explained by the decreasing rate of increase in creep and shrinkage of concrete with age.

Comparison with Code Predictions

Table 6 compares the measured beam midspan deflections upon superimposed loading at time, t=t_0 (i.e., immediate deflection) and at t=t_0+119 days (i.e., just prior to removal of the superimposed load for most of the beams) with the predicted deflections according to ACI 318[1] and Eurocode.[2] For the ACI 318 predictions, an effective moment of inertia, I_e approach (ACI 318 Equation 9-7) was used to determine the deflections due to the beam self-weight and the weight of the superimposed load block. Because the measured beam deflections were initialized (zeroed) immediately before the superimposed loading at time, t=t_0, the ACI 318 predictions were also initialized at $t = t_0$ by subtracting the estimated creep and shrinkage deflections accumulated between the end of casting at t=0 and the placement of the load block at t=t_0.

To predict the immediate plus time-dependent deflection, Δ_{t_0+119}, ACI 318 Equation 9-11 was used as a time-dependent multiplier (λ_{t_0+119}, λ_{119}, λ_{t_0}) based on each load duration. The measured material properties (e.g., E_c, E_s) were used and the uncracked section properties were based on the gross concrete section. For the CC Series beams, Δ_{t_0+119} was determined as:

$$\Delta_{t_0+119} = (1 + \lambda_{119})\Delta'_{S_i} + \lambda_{t_0+119}\Delta'_{W_i} - \lambda_{t_0}\Delta_{W_i} \quad (2)$$

$$\Delta'_{S_i} = \frac{M_S}{M_S+M_W}\Delta_{(W+S)_i} \text{ and } \Delta'_{W_i} = \frac{M_W}{M_S+M_W}\Delta_{(W+S)_i} \quad (3)$$

$$\Delta_{(W+S)_i} = \frac{(P/2)a}{24E_cI_e}\left(3{l_n}^2 - 4a^2\right) + \frac{5wl_n{}^4}{384E_cI_e} \text{ and } \Delta_{W_i} = \frac{5wl_n{}^4}{384E_cI_g} \quad (4)$$

where, Δ'_{S_i} , Δ'_{W_i} =immediate deflection from superimposed load and beam self-weight, respectively; $\Delta_{(W+S)_i}$ =immediate deflection from self-weight plus superimposed load; Δ_{W_i} = immediate self-weight deflection prior to cracking; M_S=midspan moment due to superimposed load; M_W=midspan moment due to self-weight; P=total weight of superimposed load block; a=distance from support to superimposed load application point; l_n=distance between beam end

supports; w=distributed self-weight of beam; I_e=effective moment of inertia using ACI 318 Equation 9-7 with total moment from self-weight plus superimposed load; and I_g=gross moment of inertia of concrete section. Note that Δ'_{S_i} and Δ'_{W_i} in **Eq. 3** were both calculated using I_e under the total moment from self-weight plus superimposed load; predictions based on the initial application of self-weight followed by the superimposed load (i.e., assuming $\Delta'_{W_i}=\Delta_{W_i}$ and $\Delta'_{S_i}=\Delta_{(W+S)_i}-\Delta_{W_i}$ in **Eq. 2**) resulted in little differences (approximately 5% greater deflections).

Similarly, for the UC and UT Series beams (i.e., beams designed as uncracked):

$$\Delta_{t_0+119} = (1+\lambda_{119})\Delta_{S_i} + \lambda_{t_0+119}\Delta_{W_i} - \lambda_{t_0}\Delta_{W_i} \quad (5)$$

$$\Delta_{S_i} = \frac{(P/2)a}{24E_cI_g}\left(3{l_n}^2 - 4a^2\right) \text{ and } \Delta_{W_i} = \frac{5w{l_n}^4}{384E_cI_g} \quad (6)$$

where, Δ_{S_i}=immediate superimposed load deflection. **Table 6** also gives the predictions from Eurocode,[2] which uses an effective moment of inertia for the immediate deflections of cracked beams, combined with an effective modulus of elasticity for the creep deflections. Shrinkage curvatures are also prescribed, which yield shrinkage deflections by integration. Similar to ACI 318,[1] the Eurocode predictions were initialized at the time of superimposed loading (t=t_0) by subtracting the estimated creep deflections due to beam self-weight and shrinkage from t=0 to t=t_0. Material properties were taken as the measured values and the uncracked section properties were based on the gross concrete section. Following the Eurocode procedures in Webster and Brooker,[23] the deflection, Δ_{t_0+119} for both cracked and uncracked beams was determined as:

$$\Delta_{t_0+119} = \frac{(P/2)a}{24E_{LT}I}(3{l_n}^2 - 4a^2) + \frac{5w{l_n}^4}{384E_{LT}I} + \frac{{l_n}^2}{8}\kappa_{sh,t_0+119} - \frac{5w{l_n}^4}{384E_eI_g} - \frac{{l_n}^2}{8}\kappa_{sh,t_0} \quad (7)$$

$$E_{LT} = (M_W + M_S)/(\frac{M_W}{E_{e,W}} + \frac{M_S}{E_{e,S}}) \quad (8)$$

$$E_{e,W} = \frac{E_c}{1+\phi_{t_0+119}} \text{ and } E_{e,S} = \frac{E_c}{1+\phi_{119}} \text{ and } E_e = \frac{E_c}{1+\phi_{t_0}} \quad (9)$$

where, I=I_e calculated based on Eurocode Equations 7.18 and 7.19 for the CC Series beams, and $I = I_g$ for the UC and UT Series beams; ϕ_{t_0}, ϕ_{t_0+119}, ϕ_{119}=creep coefficient according to Eurocode[2] Annex B for self-weight duration of t_0 days, self-weight duration of t_0+119 days, and superimposed load duration of 119 days, respectively; κ_{sh,t_0+119}, κ_{sh,t_0}=shrinkage curvature according to Eurocode Equation 7.21 determined at time, t=t_0+119 and t=t_0, respectively.

The results in **Table 6** are depicted in **Fig. 10**, where the shaded ranges represent the extreme ratios of predicted to measured deflection. Both ACI 318 and Eurocode generally gave good design estimates for the immediate deflections under superimposed load. The predictions were slightly better for the intentionally-cracked CC Series beams than the UT and UC Series beams. In comparison, long-term sustained-load deflections of both the NA and RCA concrete beams were significantly underestimated for the UC and UT Series. This large discrepancy may have occurred due to the cracking of the UC and UT Series beams under the creep and shrinkage deformations of the concrete over time, which was not captured by the design predictions. While cracking was not visually observed in the UT Series beams, some amount of micro-cracking likely occurred as a result of the creep and shrinkage deformations, resulting in larger deflections. For the CC Series beams, long-term deflections were somewhat underestimated by ACI 318 and overestimated by Eurocode by approximately similar percent errors. A more detailed approach (e.g., fiber or finite element modeling) that can incorporate stress redistribution under long-term creep and shrinkage effects in reinforced concrete may be needed to better predict the time-dependent deflections of the beams. An interesting finding is that the ability of the design methods to predict the measured deflections did not differ significantly between the NA concrete and RCA concrete beams. This is likely because of the use of measured concrete properties in the predictions (for example, smaller E_c for RCA concrete).

SUMMARY AND CONCLUSIONS

This paper experimentally investigated the effect of RCA on the time-dependent sustained service-load behavior of normal strength reinforced concrete beams. The important findings from the study are given below. In interpreting these findings, it should be noted that the results may be limited to the materials and specimens tested.

1. Increased R results in increased immediate and long-term sustained-load deflections of reinforced concrete beams. While the goal is to maximize the use of RCA (i.e., R=100%), the increased deflections should be quantified to ensure that allowable deflection limits are satisfied.

2. Similar to NA concrete, sustained-load deflections of RCA concrete beams are affected by loading age, presence of compression reinforcement, and amount of cracking. Beams loaded at 7 days tended to have larger long-term deflections than beams loaded at 28 days. Beams with compression steel had reduced long-term deflections than beams without compression steel.

3. The effect of RCA on deflections is smaller for beams with increased cracking. For example, at approximately four months of loading, beams that were not intentionally cracked under the initial application of superimposed load experienced a deflection increase of approximately 49% from the R=0% case (i.e., NA concrete) to the R=100% case. In comparison, beams that were intentionally cracked under the initial application of superimposed load showed an increase of approximately 21% from R=0% to R=100%.

4. Increased amounts of RCA lead to increased cracking in reinforced concrete beams as a result of the decreased modulus of rupture of RCA concrete.

5. Creep and shrinkage strains result in a significant downward shift of the neutral axis (location of zero total strain) in reinforced concrete beams. This effect is greater in RCA concrete beams than in NA concrete beams because of the increased creep and shrinkage deformations of

RCA concrete. The increase in the neutral axis depth is greater for beams loaded at 7 days as compared to beams loaded at 28 days. This trend can be explained by considering the decreasing rate of change of creep and shrinkage as the concrete ages.

6. ACI 318[1] and Eurocode[2] procedures resulted in reasonable predictions for the immediate deflections of the NA and RCA concrete beam test specimens.

7. In comparison, the long-term deflections were significantly underestimated when applying ACI 318 and Eurocode procedures on the NA and RCA concrete specimens that were not intentionally cracked under the initial application of superimposed load. This large discrepancy may have occurred due to the cracking of these beams under the creep and shrinkage deformations of concrete over time, which were not captured by the design predictions.

8. For the specimens that were cracked under the initial application of superimposed load, the long-term deflections were somewhat underestimated by ACI 318 and overestimated by Eurocode by approximately similar percent errors.

9. The ability of ACI 318 and Eurocode to predict the measured deflections was similar for the NA concrete and RCA concrete beams. This may be because measured concrete properties were used in the predictions (e.g., smaller modulus of elasticity for RCA concrete).

ACKNOWLEDGMENTS

Partial funding for this work was provided by the National Science Foundation (NSF) under Grant No. CMMI 1436758. The support of the NSF Program Director, Dr. K.I. Mehta, is gratefully acknowledged. The authors thank the Sika Corporation and Transit Mix South Bend for material donations and Dave Schelling of the LaPorte district INDOT office for L.A. abrasion testing. Any findings, conclusions, or recommendations in the paper are those of the authors and do not necessarily represent the views of the NSF or the individuals/organizations listed.

REFERENCES

1. ACI Committee 318, "Building Code Requirements for Structural Concrete and Commentary," American Concrete Institute, Farmington Hills, MI, 2011.
2. British Standards Institution, "Eurocode 2: Design of Concrete Structures. General Rules and Rules for Buildings," BS EN 1992-1-1, 2004.
3. Knaack, A., Kurama, Y, "Sustainable Concrete Structures using Recycled Concrete Aggregate: Short-Term and Long-Term Behavior Considering Material Variability," *NDSE Report 13-01*, 2013, Univ. of Notre Dame, *www.nd.edu/~concrete/RCA-concrete/*.
4. Ajdukiewicz, A., Kliszczewicz, A., "Long-Term Behavior of Reinforced-Concrete Beams and Columns Made of Recycled Aggregate Concrete," *fib Symposium*, Prague, Czech Republic, 2011, 479-482.
5. Choi, W., Yun, H., "Long-term Deflection and Flexural Behavior of Reinforced Concrete Beams with Recycled Aggregate," *Materials & Design*, 51, 2013, 742-750.
6. Lapko, A., Grygo, R., "Long Term Deflection of Recycled Aggregate Concrete (RAC) Beams Made of Recycled Concrete," *10th International Conference: Modern Building Materials, Structures and Techniques*, Vilnius, Lithuania, 2010.
7. Sato, R., Maruyama, I., Sogabe, T., Sogo, M., "Flexural Behavior of Reinforced Recycled Concrete Beams," *J. of Advanced Concrete Technology*, 5(1), 2007, 43-61.
8. Li, X., "Recycled and Reuse of Waste Concrete in China Part II: Structural Behavior of Recycled Aggregate Concrete and Engineering Applications," *Resources, Conservation and Recycling*, 53(3), 2009, 107-112.
9. ACI Committee 555, "Removal and Reuse of Hardened Concrete," American Concrete Institute, 2001, Farmington Hills, MI.

10. Domingo-Cabo, A., Lázaro, C., López-Gayarre, F., Serrano-López, M., Serna, P., Castaño-Tabares, J., "Creep and Shrinkage of Recycled Aggregate Concrete," *Construction and Building Materials*, 23(3), 2009, 2545-2553.
11. Fathifazl, G., Abbas, A., Razaqpur, A., Isgor, O., Foo, S., "New Mixture Proportioning Method for Concrete Made with Coarse Recycled Concrete Aggregate," *J. of Materials in Civil Engineering*, 21(10), 2009, 601-611.
12. Hansen T., "Recycled Aggregates and Recycled Aggregate Concrete Second State-of-the-Art Report Developments 1945-1985," *Materials and Structures*, 19(3), 1986, 201-246.
13. Kerkhoff, B., Siebel, E., "Properties of Concrete with Recycled Aggregates," *Beton 2/2001*, 2001, 47-58.
14. Knaack, A., Kurama, Y., "Design of Concrete Mixtures with Recycled Concrete Aggregates," *ACI Materials J.*, 110(5), 2013, 483-494.
15. Yamato, T., "Mechanical Properties, Drying Shrinkage and Resistance to Freezing and Thawing of Concrete using Recycled Aggregate," *ACI SP-179*, 1998, 103-121.
16. Fathifazl, G., Razaqpur, A., "Creep Rheological Models for Recycled Aggregate Concrete," *ACI Materials J.*, 110(2), 2013, 115-125.
17. Fathifazl, G., Razaqpur, A., Isgor, O., Abbas, A., Fournier, B., Foo, S., "Creep and Drying Shrinkage Characteristics of Concrete Produced with Coarse Recycled Concrete Aggregate," *Cement & Concrete Composites*, 33(10), 2011, 1026-1037.
18. Domingo, A., Lázaro, C., Gayarre, F., Serrano, M., Lopez-Colina, C., "Long Term Deformations by Creep and Shrinkage in Recycled Aggregate Concrete," *Materials and Structures*, 43(8), 2010, 1147-1160.
19. INDOT, "Standard Specifications," 2012, Indiana Department of Transportation.

20. ASTM International, *Annual Book of ASTM Standards*, 2009, Philadelphia, PA.

21. Abbas, A., Fathifazl, G., Isgor, O.B., Razaqpur, A.G., Fournier, B., Foo, S., "Proposed Method for Determining the Residual Mortar Content of Recycled Concrete Aggregates," *J. of ASTM International*, 5(1), 2008, 1-12.

22. Kosmatka, S., Kerkhoff, B., Panarese, W., "Design and Control of Concrete Mixtures," Portland Cement Association, 14th Edition, Skokie, IL, 2002.

23. Webster, R., Brooker, O., "How to Design Concrete Structures Using Eurocode 2: Deflection Calculations," The Concrete Centre, 2006, 8 pp.

TABLES

Table 1 – Natural aggregate and recycled concrete aggregate properties

Aggregate ID	Type/ Source Location	Specific Gravity			Water Absorption, A_{na} or A_{rca} (%Weight)	Res. Mortar Content, RM_{rca} (%Weight)	Deleterious Mat. Cont., D_{rca} (%Weight)	Gradation	L.A. Abrasion Loss (%Weight)
		Bulk Dry	SSD	App.					
FA	Concrete Sand	2.59	2.63	2.69	1.39	-	-	INDOT #23	-
NA-CL	Crushed Limestone	2.71	2.73	2.76	0.74	-	-	INDOT #8	21.0
RCA-S	South Bend, IN	2.18	2.32	2.52	6.06	30.4	5.68	INDOT #8	37.8

Table 2 – Dry-weight proportions of concrete mix designs

Replacement, *R* (%)	**Water[1] (kg/m^3)**	**Cement (kg/m^3)**	**NA (kg/m^3)**	**RCA (kg/m^3)**	**FA[2] (kg/m^3)**	**HRWR[3] (mL/m^3)**	**AEA[4] (mL/m^3)**
0 (NAC)	150	341	1137	-	676	1874	314
50 (RCA-50)	150	341	568	458	676	1874	314
100 (RCA-100)	150	341	-	917	676	1874	314

Notes: 1 lb/yd^3=0.5933 kg/m^3; 1 fl.oz./yd^3=38.67 mL/m^3.
[1]Amount of mix water required beyond saturated surface dry condition of coarse and fine aggregates.
[2]Fine Aggregate. [3]High Range Water Reducer. [4]Air Entraining Agent.

1

Table 3 – Beam test specimen details

Beam ID	P (kN)	R (%)	t_0 (days)	ρ_s (%)	ρ'_s (%)	ρ_t (%)	Date Loaded	Date Unloaded	Total Load Duration
UT-0-28	3.63	0	28	1.32	--	--	1/17/12	5/15/12	119
UT-0-7	3.64	0	7	1.32	--	--	1/25/12	5/23/12	119
UC-0-28	3.63	0	28	1.32	0.47	0.987	10/8/12	3/27/13	170
UC-0-7	3.64	0	7	1.32	0.47	0.987	6/6/12	10/3/12	119
CC-0-28	9.54	0	28	1.32	0.47	0.987	6/5/12	10/2/12	119
CC-0-7*	9.51	0	7	1.32	0.47	0.987	10/17/12	5/31/13	226
UT-50-28	3.63	50	28	1.32	--	--	1/17/12	5/15/12	119
UT-50-7	3.63	50	7	1.32	--	--	6/6/12	10/3/12	119
UC-50-28	3.64	50	28	1.32	0.47	0.987	10/8/12	3/27/13	170
UC-50-7*	3.63	50	7	1.32	0.47	0.987	10/17/12	5/31/13	226
CC-50-28	9.51	50	28	1.32	0.47	0.987	6/5/12	10/2/12	119
CC-50-7	9.51	50	7	1.32	0.47	0.987	1/25/12	5/23/12	119
UT-100-28	3.63	100	28	1.32	--	--	6/5/12	10/2/12	119
UT-100-7	3.64	100	7	1.32	--	--	6/6/12	10/3/12	119
UC-100-28	3.64	100	28	1.32	0.47	0.987	10/8/12	3/27/13	170
UC-100-7	3.64	100	7	1.32	0.47	0.987	1/25/12	5/23/12	119
CC-100-28	9.54	100	28	1.32	0.47	0.987	1/17/12	5/15/12	119
CC-100-7*	9.54	100	7	1.32	0.47	0.987	10/17/12	5/31/13	226

$\rho_s = A_s/bd$ and $\rho'_s = A'_s/bd$, where A_s, A'_s =tension and compression steel areas, respectively, b =beam width, and d =effective depth to tension reinforcement; $\rho_t = n_{tr}A_{tr}/bl$, where n_{tr} =number of stirrups, A_{tr} =total vertical leg area of one stirrup, and l =full beam length.

*Last 56 days of loading for Beams CC-0-7, CC-100-7, and UC-50-7 included an additional small weight block that was placed on top of the original block.

Table 4 – Concrete material properties

Beam ID	Mini Slump (mm)	Unit Wt. (kg/m^3)	t=7 Days			t=28 Days			t=90 Days	
			E_c (GPa)	f'_c (MPa)	f'_t (MPa)	E_c (GPa)	f'_c (MPa)	f'_t (MPa)	E_c (GPa)	f'_c (MPa)
UT-0-28	57.2	2230	--	--	--	29.4	32.6	4.19	--	--
UT-0-7	31.8	2419	36.3	46.6	5.03	34.4	50.3	--	33.1	47.4
UC-0-28	44.5	2403	40.7	46.0	--	38.7	49.3	5.36	39.7	49.2
UC-0-7	44.5	2295	33.5	37.2	4.20	35.0	42.0	--	33.9	38.7
CC-0-28	63.5	2265	35.3	36.7	--	31.4	40.2	4.50	33.2	36.7
CC-0-7	50.8	2392	38.0	42.5	3.97	39.1	46.5	--	35.4	47.5
UT-50-28	50.8	2284	--	--	--	29.4	43.6	4.41	--	--
UT-50-7	57.2	2263	28.6	38.6	4.21	31.0	40.2	--	28.2	39.0
UC-50-28	38.1	2334	31.6	44.3	--	33.8	49.6	4.39	30.3	46.0
UC-50-7	50.8	2313	33.0	41.0	3.32	27.6	43.6	--	28.8	44.0
CC-50-28	76.2	2243	27.8	36.2	--	27.8	37.7	4.11	27.1	39.9
CC-50-7	63.5	2243	26.9	38.0	3.42	28.8	40.0	--	26.6	40.7
UT-100-28	76.2	2174	23.3	38.6	--	23.3	41.4	3.85	23.4	38.6
UT-100-7	57.2	2209	22.8	36.2	3.55	22.3	35.7	--	20.8	35.5
UC-100-28	38.1	2243	25.2	42.2	--	25.8	48.2	3.71	23.7	45.3
UC-100-7	57.2	2178	23.4	38.8	3.47	22.8	40.6	--	21.7	41.6
CC-100-28	50.8	2162	--	--	--	23.3	43.8	3.43	--	--
CC-100-7	63.5	2170	22.7	37.5	2.79	21.6	38.5	--	20.4	37.8

Note: 1 lb/ft^3=16.0 kg/m^3; 1 ksi=6.89 MPa.
Mini slump measured as described in Knaack and Kurama.[14] Unit weight measured by weighing modulus of rupture (MOR) beams at age of loading. E_c= modulus of elasticity; f'_c=compressive strength; f'_t=tension strength (MOR).

1

Table 5 – Reinforcing steel properties in tension

Bar Size	E_s **(GPa)**	f_y **(MPa)**	ϵ_y	f_u **(MPa)**	ϵ_u	ϵ_f
No. 10	198	443	0.00290	732	0.0971	0.128
No. 16	197	572	0.00360	706	0.0882	0.131
Notes: 1 ksi=6.89 MPa. E_s=modulus of elasticity; f_y=yield strength; ϵ_y=yield strain; f_u=ultimate (peak) strength; ϵ_u=strain at ultimate strength; ϵ_f=fracture strain at stress, f_f=0.80f_u.						

1

Table 6 – Measured and predicted beam deflections

Beam ID	Immediate Superimposed Load Deflection at t=t_0, Δ'_{S_i} (mm)			Sustained Long-Term Deflection at t=t_0+119, Δ_{t_0+119} (mm)		
	Measured	ACI 318[1]	Eurocode[2]	Measured	ACI 318[1]	Eurocode[2]
UT-0-28	0.86	0.79	0.79	5.00	1.91	2.69
UT-0-7	0.74	0.71	0.71	4.62	1.70	2.31
UC-0-28	0.66	0.61	0.61	3.51	1.30	1.60
UC-0-7	0.94	0.71	0.71	5.11	1.60	2.90
CC-0-28	3.15	3.71	3.20	10.19	7.29	11.81
CC-0-7	3.40	3.71	3.10	10.69	7.49	13.49
UT-50-28	0.91	0.79	0.79	5.38	1.91	2.31
UT-50-7	0.94	0.79	0.79	6.96	2.11	3.30
UC-50-28	0.86	0.71	0.71	4.70	1.50	1.91
UC-50-7	0.84	0.71	0.71	5.99	1.60	2.79
CC-50-28	4.93	4.29	3.71	n/a	8.41	13.59
CC-50-7	4.14	4.80	4.19	12.90	9.60	17.70
UT-100-28	1.24	0.99	0.99	7.39	2.39	3.00
UT-100-7	1.12	1.09	1.09	n/a	2.59	4.29
UC-100-28	0.97	0.89	0.89	5.94	1.91	2.49
UC-100-7	1.27	0.99	0.99	7.62	2.31	3.99
CC-100-28	5.11	5.11	4.50	12.27	10.01	14.10
CC-100-7	4.60	5.41	4.90	14.68	10.90	19.81
Note: Δ'_{S_i}=Δ_{S_i} for UC and UT Series beams. n/a=not available.						

1

FIGURES

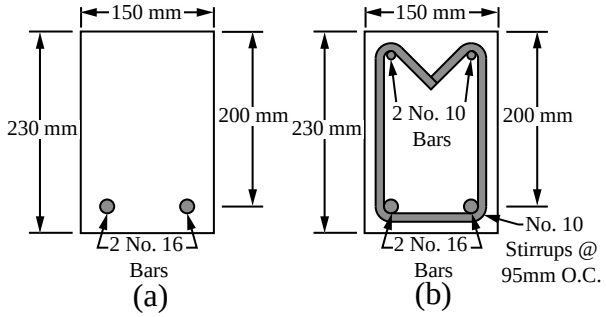

Figure 1 – Beam specimens: (a) without compression or transverse steel (UT Series); (b) with compression and transverse steel (UC and CC Series)

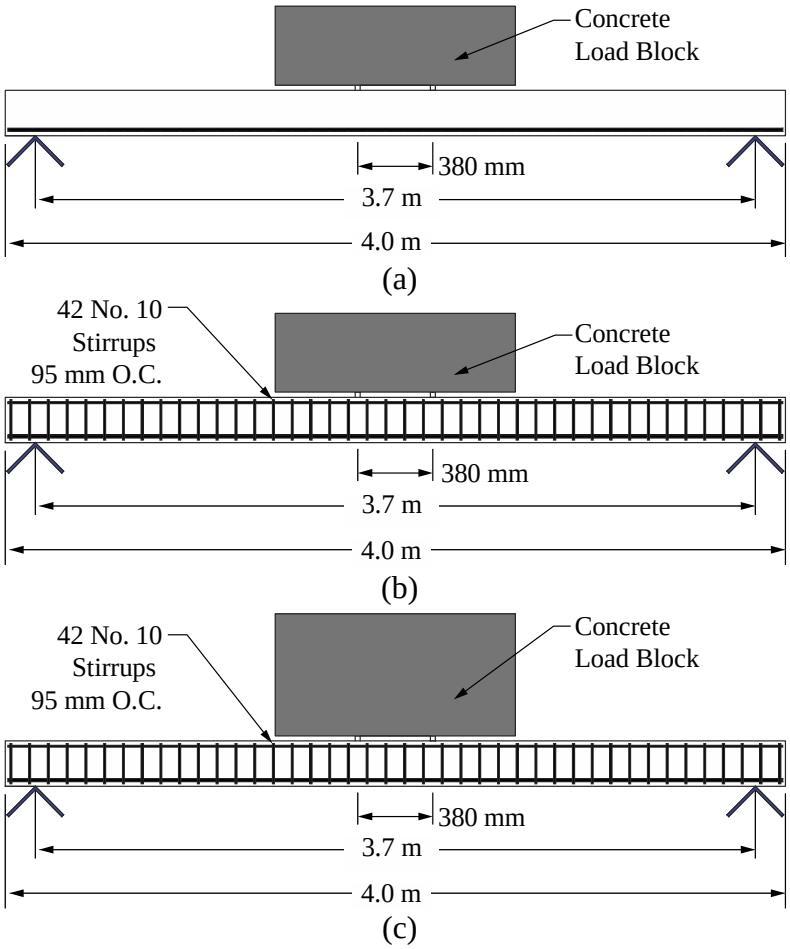

Figure 2 – Beam test elevation: (a) UT Series beams; (b) UC Series beams; (c) CC Series beams

1

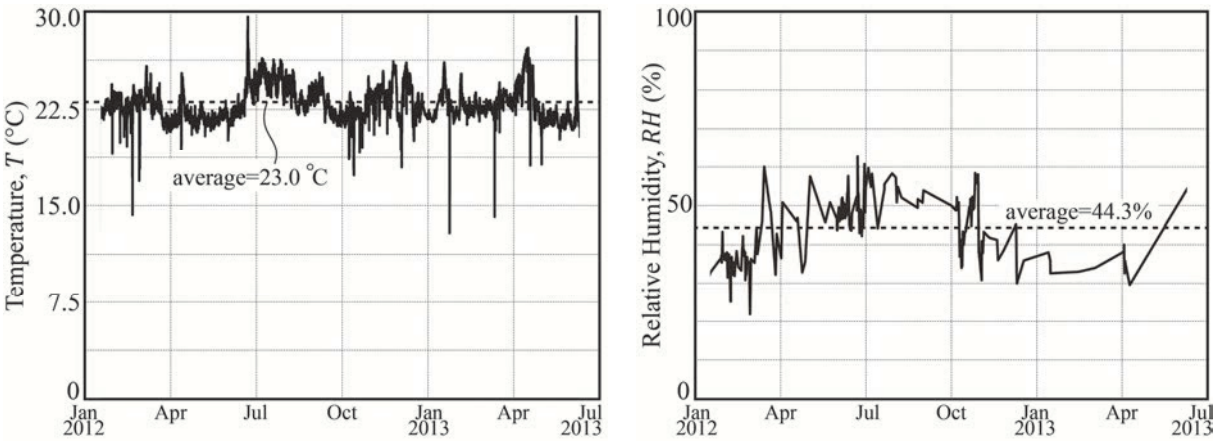

(a) (b)

Figure 3 – Laboratory environmental conditions: (a) temperature; (b) humidity

1

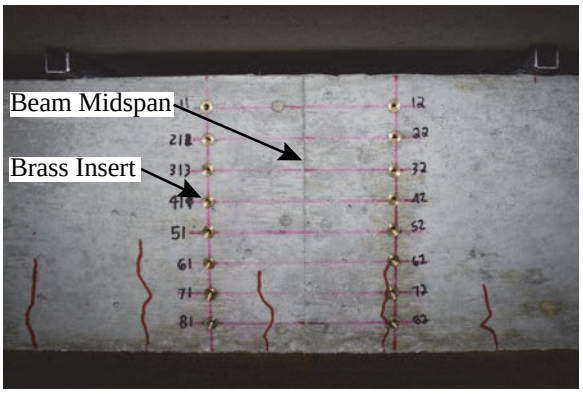

Figure 4 – Beam elevation view with brass inserts near midspan

1

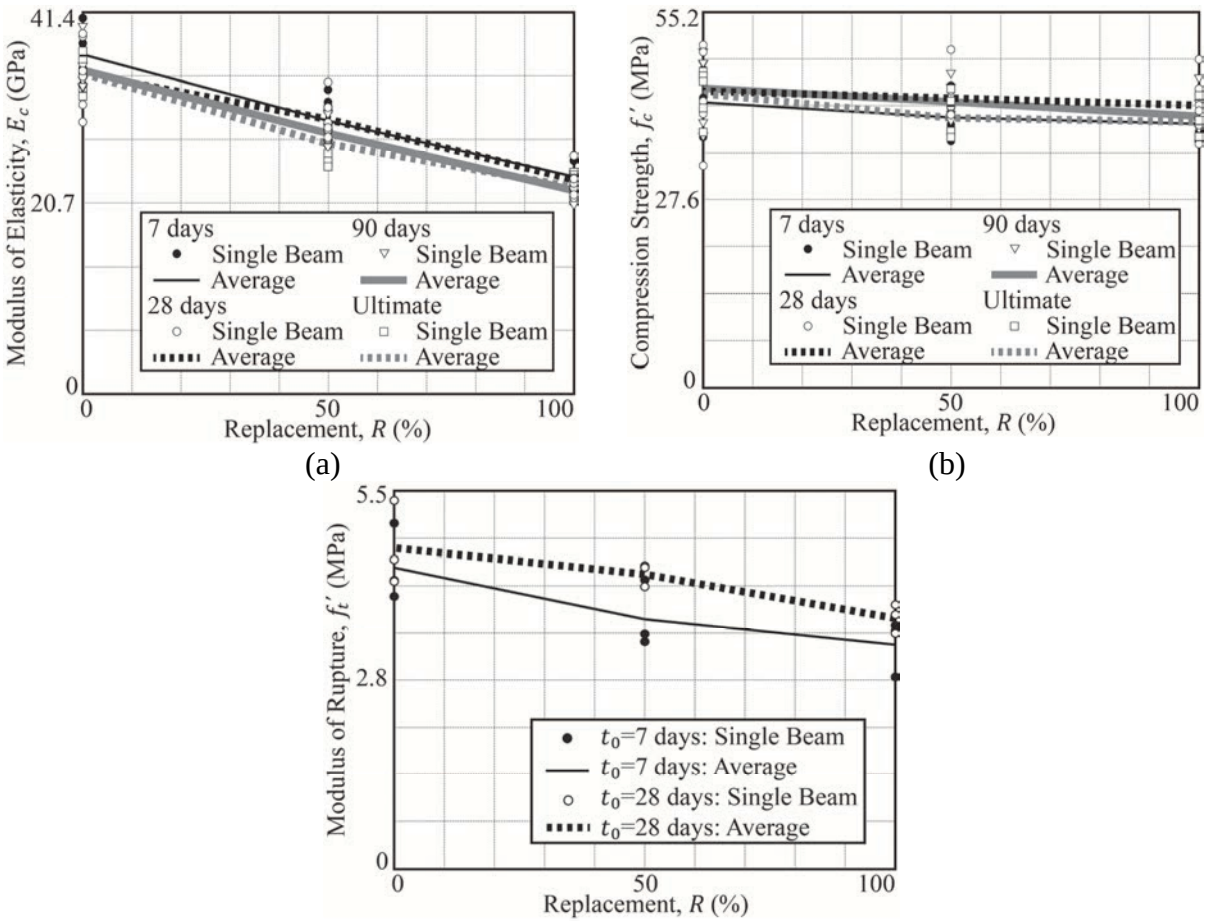

Figure 5 – Beam concrete properties: (a) modulus of elasticity, E_c; (b) compression strength, f_c'; (c) tension strength, f_t'

1

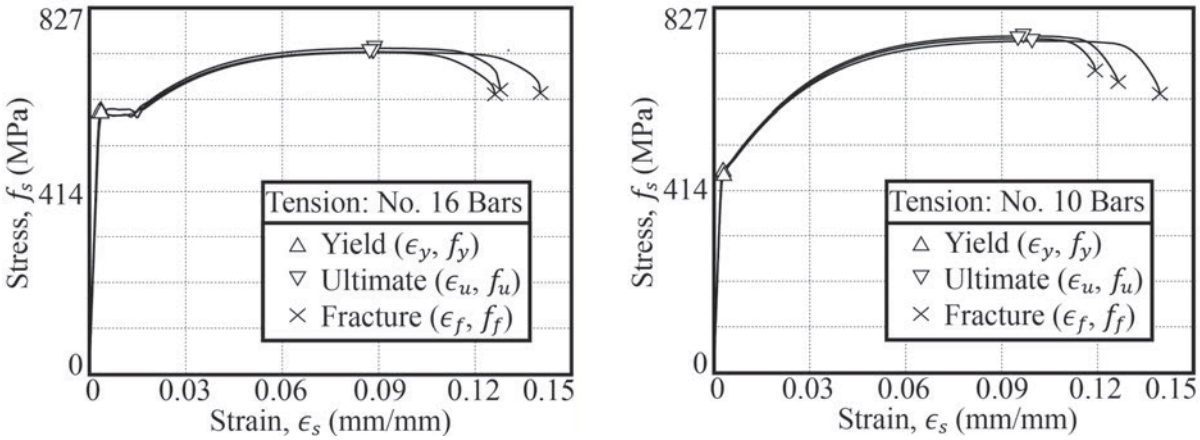

(a) (b)

Figure 6 – Behavior of reinforcing steel: (a) No. 16 bars; (b) No. 10 bars

1

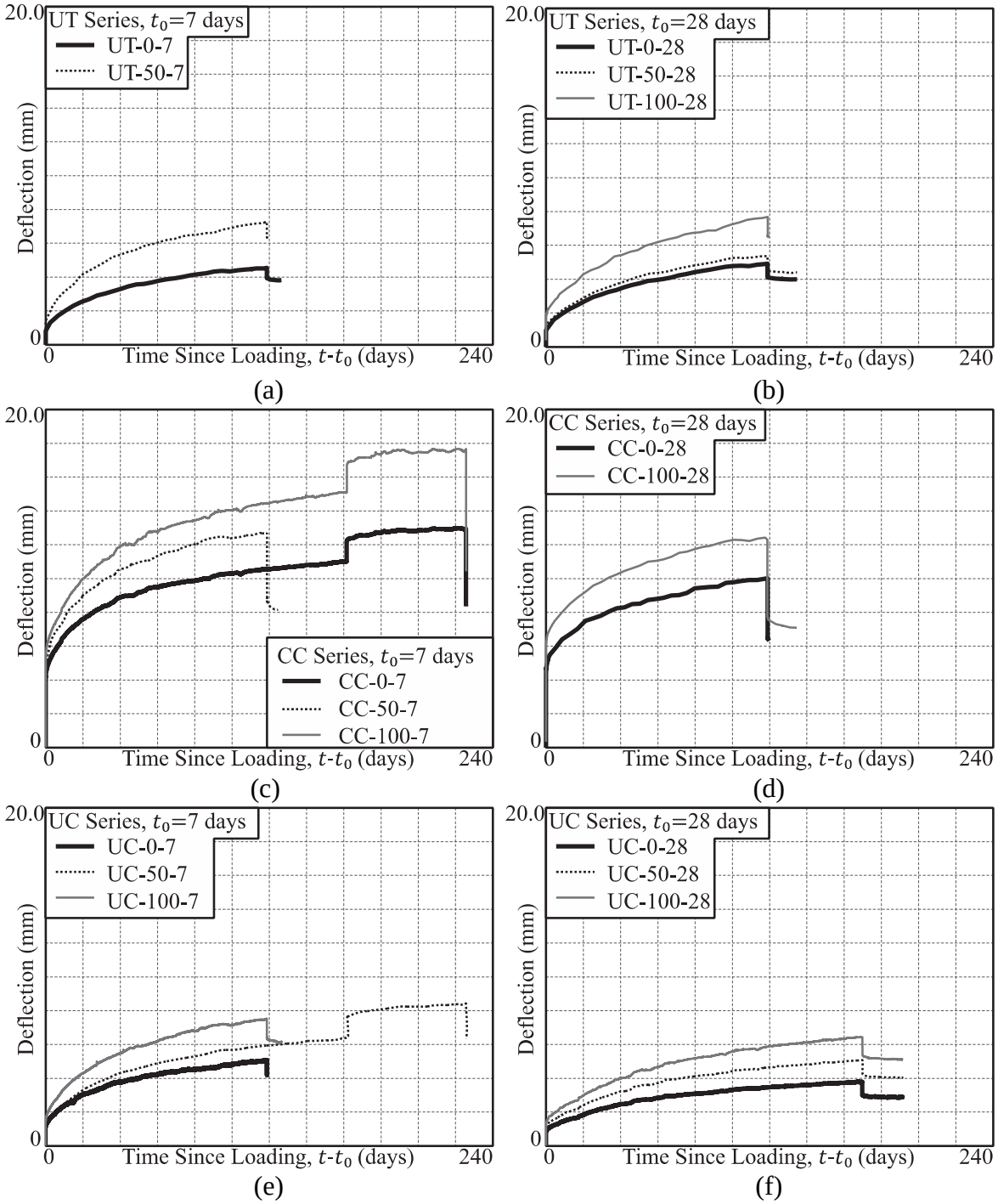

Figure 7 – Beam midspan deflections: (a) t_0=7 days, UT Series, ρ'_s=0%; (b) t_0=28 days, UT Series, ρ'_s=0%; (c) t_0=7 days, CC Series, ρ'_s=0.47%; (d) t_0=28 days, CC Series, ρ'_s=0.47%; (e) t_0=7 days, UC Series, ρ'_s=0.47%; (f) t_0=28 days, UC Series, ρ'_s=0.47%

1

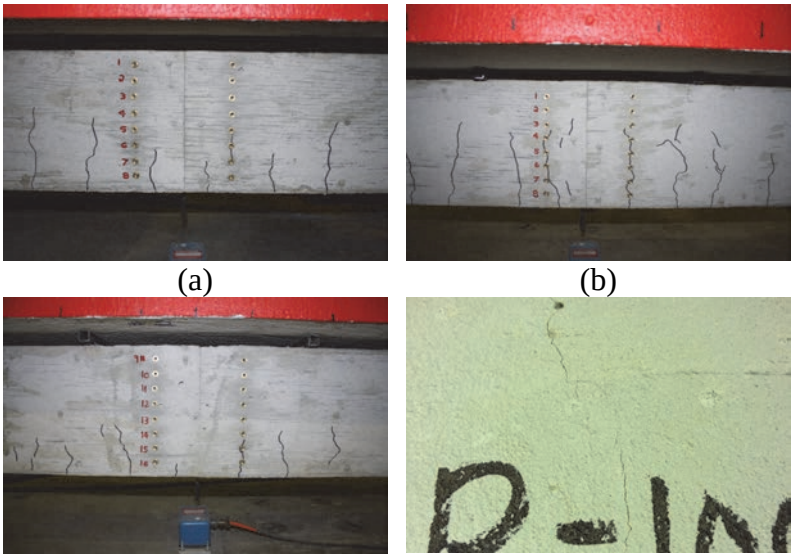

(a) (b)

(c) (d)

Figure 8 – Beam cracking [note that the cracks were hairline; but, they have been highlighted for easier viewing in Figs. 8(a-c)]: (a) flexural cracking on CC-0-7; (b) flexural cracking on CC-100-7; (c) flexural cracking on UC-50-7; (d) shrinkage cracking on top surface of UC-100-28

1

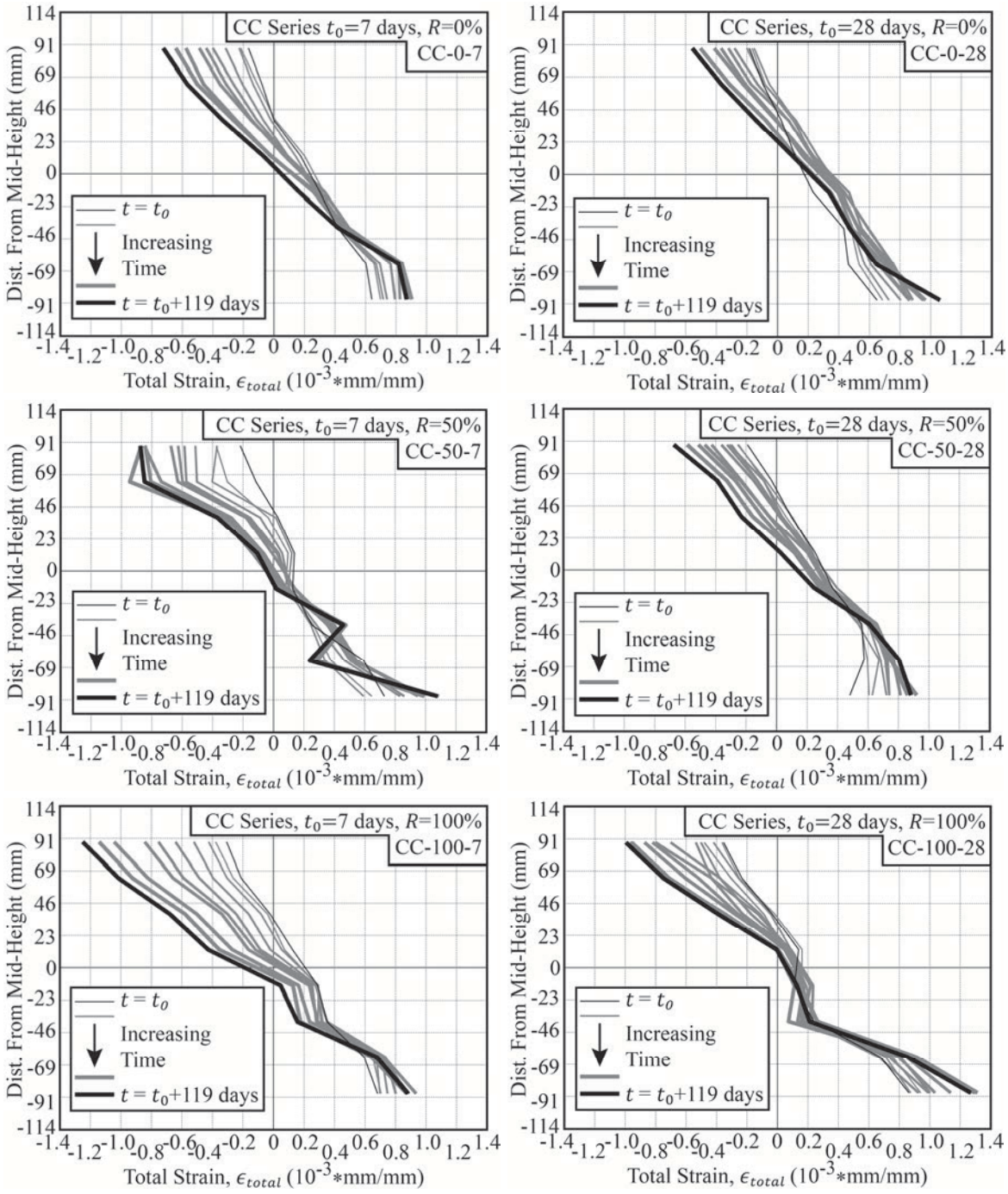

Figure 9 – Total strain diagrams over height of CC Series beams [R=0% (top), 50% (middle), and 100% (bottom)]: (a) t_0=7 days; (b) t_0=28 days

1

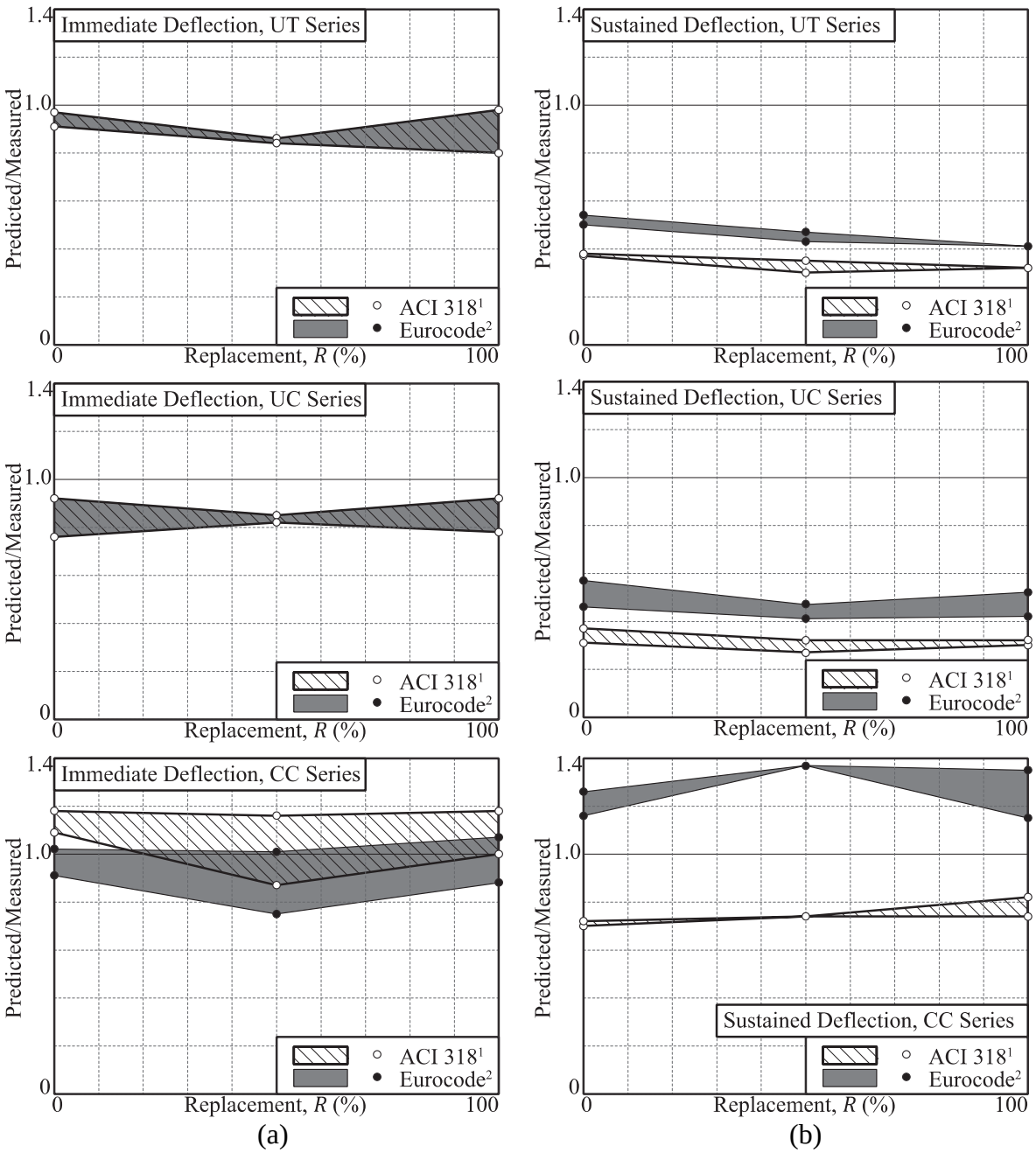

Figure 10 – Measured versus predicted beam midspan deflections [UT Series (top), UC Series (middle), and CC Series (bottom)]: (a) immediate deflection at t=t_0; (b) sustained long-term deflection at t=t_0+119 days

1